

Article

Terrace Morpho-Sedimentary Sequences on the Sibari Plain (Calabria, Southern Italy): Implication for Sea Level and Tectonic Controls

Federica Lucà ^{1,*}, Andrea Brogno ¹, Vincenzo Tripodi ² and Gaetano Robustelli ¹

¹ Department of Biology, Ecology and Earth Science (DiBEST), University of Calabria, 87036 Rende, Italy; andrea.brogno91@gmail.com (A.B.); gaetano.robustelli@unical.it (G.R.)

² National Research Council of Italy—Research Institute for Geo-Hydrological Protection (IRPI), 87036 Rende, Italy; vincenzo.tripodi@irpi.cnr.it

* Correspondence: federica.luca@unical.it

Abstract: The Sibari Plain (northeastern Calabria) shows a well-developed stair of late Quaternary marine/coastal terraces resulting from the interaction between sea level fluctuations and tectonic uplift. This paper (i) provides a stratigraphic description of terraced deposits between the Raganello and Coscile rivers, (ii) assesses the relative controls of eustasy and uplift on the staircase formation, and (iii) unravels the Quaternary morphosedimentary evolution of the study area. A geomorphological approach was coupled with stratigraphic field surveys. Photo interpretation, topographic map analyses, and field surveys allowed us to map ten orders of terraces forming telescopically incised valley-fills. Based on the uppermost position of foreshore deposits on inner margins and an average uplift rate of ~1 mm/y, inferred from the Marine Isotope Stage (MIS) 5.5, terraces were correlated with highstands. Sedimentological and stratigraphic analyses allowed us to recognize four assemblages of genetically associated sedimentary facies related to superimposed and juxtaposed coastal and alluvial systems, showing a seaward-stepping architecture. Based on stratal geometry and facies association, we argue that alluvial/fluvial sediments and coastal depositional systems formed contemporaneously along the same terrace. Terrace arrangement resulted from repeated cycles of valley incision (sea level fall) and aggradational to progradational stacking pattern (sea level rise and highstands) in a framework of sustained uplift.

Keywords: marine terraces; morphostratigraphic correlations; late quaternary; relative sea level; Sibari Plain; Calabria



Citation: Lucà, F.; Brogno, A.; Tripodi, V.; Robustelli, G. Terrace Morpho-Sedimentary Sequences on the Sibari Plain (Calabria, Southern Italy): Implication for Sea Level and Tectonic Controls. *Geosciences* **2022**, *12*, 211. <https://doi.org/10.3390/geosciences12050211>

Academic Editors: Angelos G. Maravelis and Jesus Martinez-Frias

Received: 31 March 2022

Accepted: 10 May 2022

Published: 16 May 2022

Publisher's Note: MDPI stays neutral with regard to jurisdictional claims in published maps and institutional affiliations.



Copyright: © 2022 by the authors. Licensee MDPI, Basel, Switzerland. This article is an open access article distributed under the terms and conditions of the Creative Commons Attribution (CC BY) license (<https://creativecommons.org/licenses/by/4.0/>).

1. Introduction

The presence of remarkable flights of marine terraces is characteristic of the Ionian coast of southern Apennine, from Basilicata to Calabria. This geomorphological setting is the result of interaction between the dominant tectonic uplift trend and eustatic sea level changes.

The flights of uplifted terraces occur along the frontal thrust belt of the southern Apennines and provide the best constraint to evaluate long-term uplift rates [1,2]. However, a variable amount of uplift characterizes the Ionian southern Apennine coast. The vertical and lateral distribution of the terraces shows a general northeastward tilt of northern Calabria, but coast-parallel profiles of terraces also indicate local km-scale undulations (fault-induced deformations) superimposed on the regional uplift [3–8]. Previous studies ([7] and references therein) have mostly dealt with morphotectonic analysis of marine terrace flights in order to identify constraints on late Quaternary deformation of the southern Apennines orogen. Conversely, only a few studies have focused on the geomorphological/stratigraphical evolution of coastal sectors with the aim to understand its tectonic implications [6,9,10]. Further, many coastal terraces comprise marine and fluvial facies,

which, along with morphostratigraphic relationships, may be crucial for the interpretation of the driving mechanism of the terrace staircase [10,11].

This paper presents the results of an integrated stratigraphic and geomorphological approach of uplifted Middle–Late Pleistocene terraces northward of the Sibari Plain (Calabria, southern Italy). In particular, this study aims to (i) detail the stratigraphic architecture of sedimentary successions of the terraced deposits outcropping between the Coscile and Raganello rivers through facies analysis; (ii) describe terrace staircase morphology and correlation, by investigating the lateral and vertical trends of clastic sediments and their cross-cut relationships; and (iii) provide insights into the Quaternary morphosedimentary evolution of the study area by analyzing the interplay between tectonic uplift and landscape dynamics. Facies distribution and arrangement, depositional architecture, and cross-cut relationships between terraced successions were focused on to unravel the interplay between eustatic sea level fluctuations and tectonic uplift and the effect on terrace formation, as well as the influence of along-strike variation in fault-controlled subsidence on stacking patterns of terraced sediments.

2. Tectonic Background

2.1. Regional Setting

The southern Apennines are a northeast-verging fold and thrust belt (Figure 1), built on the western border of the African–Apulian plate during the Neogene. The wedge is mainly composed of Mesozoic and Cenozoic basinal and carbonate platform rocks [12] tectonically overlain by the Mesozoic Ligurian oceanic crust and relics of the innermost crystalline units of the Calabride Complex [13]. Growth of the southern Apennines occurred in the Neogene W-directed and E-retreating Adriatic–Ionian subduction zone [14], which resulted in migrating foreland and thrust–top basins (Figure 1; [13,15]).

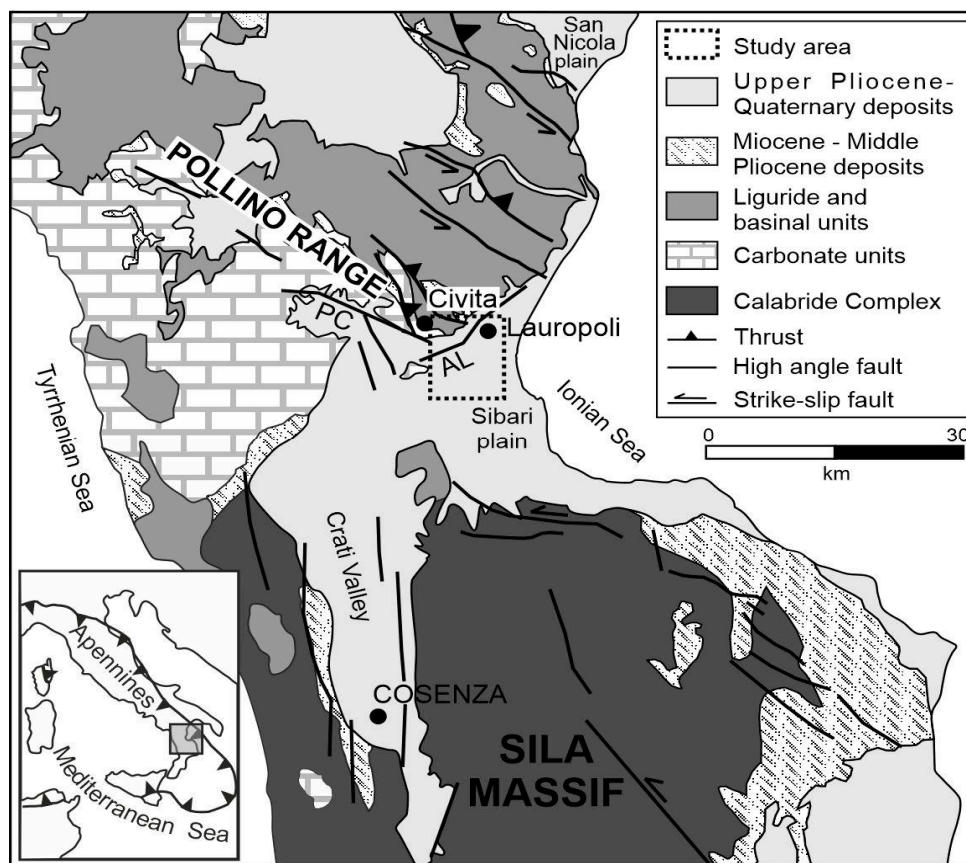


Figure 1. Geological sketch-map of southern Apennines and northern Calabria (modified after [6]). Fault system: PC: Pollino–Castrovillari; AL: Avena–Lauroполи.

The thrusting in the frontal eastern part of the accretionary wedge ceased during the Early Pleistocene. The progressive increase in continental collision and the consequent clockwise rotation of the Calabrian belt [16–18] induced the activation of transpressional faults breaking through the accretionary wedge [13,19].

Shortening in the frontal zone is still ongoing and is documented by paleo-shoreline undulations, superimposed on the regional uplift process [5–8].

The frontal belt of the southern Apennines belt has indeed experienced uplift (~1 mm/y) since the Middle Pleistocene. Uplift and sea-level changes caused the development of flights of marine terraces. In particular, raised marine shorelines associated with the MIS 5.5 highstand, dated at ~124 ky, are a key issue in constraining the regional uplift pattern [1,2].

2.2. Geological Setting

The study area is located in northern Calabria, behind the thrust front of the southern Apennines (Figure 1), which were involved in high-angle strike-slip and extensional tectonics since the early Pliocene [13,19]. Since that time, the area was filled with several hundred meters of upper Pliocene–Lower Pleistocene marine deposits [20]. The backbone of the study area is composed of Lower Pleistocene clastic deposits (Lauropoli Conglomerates in [21]; Serra dell’Ospedale Conglomerates in [22]) onto which Middle Pleistocene to Holocene marine and terrestrial deposits rest erosively and are arranged in several orders of terraces [4–7].

The southwestern side of the Pollino range is bordered by the active, WNW striking Pollino–Castrovillari fault system [23–25] and by the Civita shear zone [12] at its southeastern edge. The northwestern side of the Sibari Plain is bounded by the ENE-striking Avena–Lauropoli fault system, considered to be a dip-slip extensional structure [26].

The present-day landscape is the result of the uplift active since the middle Pleistocene, which is spectacularly documented by flights of marine terraces. Indeed, along the 70 km of coastline from the San Nicola and Sibari Plains, several marine terraces form a staircase between the present sea-level and ~650 m a.s.l. (above sea level). In particular, raised marine shorelines indicate non-uniform uplift rates moving southeastward [4,5,7,8].

Based on recent dating of raised shorelines [4,6] and references therein, the terrace located between ~100 and ~130 m in elevation was assigned to the MIS 5.5 and aged at 124 ky. The relative chronological correlations between the marine terraces and the Quaternary eustatic highstands were indirectly provided by the average uplift rate inferred from the MIS 5.5 (~1 mm/y). In the last two decades, several authors pointed out the presence of more orders of marine terraces, but a certain disagreement still exists not only on the number of terraces but also on their age and—in some cases—on their altitude a.s.l. Based on Amino Acid Racemization (AAR) datings, ref. [4] mapped four terraces along the northern side of the Sibari Plain between 75 and 340 m a.s.l. and highlighted the role of the Pollino–Castrovillari fault. Using new and existing radiometric data for marine terraces, ref. [6] recognized 11 orders of Middle Pleistocene terraces in north-eastern Calabria, but only six in the Lauropoli area. In this area, ref. [7] mapped five terraces and assigned the fourth terrace (T4) to the MIS 5.5 at 124 ky (Table 1). The MIS 5.5 terrace is the widest within the terrace flight and has the same inner margin as the T5 terrace in [6], but it is younger in age. This also results in a different chronological framework reconstructed for marine terrace flights.

Table 1. Synoptic table of marine terrace chronology in northeastern Calabria based on a critical review of all available dating. For each work, the study area, terrace order, elevation range, and corresponding Marine Isotope Stage (MIS) are listed. Data related to MIS 5.5 are shown in bold.

Paper	Study Area	Terrace Data												
		Terrace order	T1	T2	T3	T4	T5	T6	T7	T8	T9	T10		
[3]	Pollino area	Elevation (m)	12–20	60–80	85–135	115–175	170–235	220–340					420	
		MIS	1	5.1	5.3	5.5	7	9					15	
[4]	Lauropoli	Terrace order			T1	T2	T3					T4		
		Elevation (m)			75–80	115–120	115–175					340		
		MIS			5.3	5.5	7					9		
[6]	Lauropoli	Terrace order				T4	T5	T6	T7			T8	T10	
		Elevation (m)				94–112	120–125	200–225	285–290			340	445	
		MIS				5.5	7.1	7.3	7.5			9.1	9.5	
[7]	Sibari Plain	Terrace order				T4	T5		T6				T7	T8
	Lauropoli	Elevation (m)				90–125	143–215		180–295				215–350	260–445
		Elevation (m)				120	210–220		~290				~350	~450
		MIS				5.5	7.1		7.5				9.5	11
This work		Terrace order	T1	T2	T3	T4	T5	T6	T7	T8		T9	T10	
		Elevation (m)	?	65	90–100	115–120	170–175	185–195	210–215	235–245		290–310	340–35	
		MIS	?	5.1	5.3	5.5	7.1	7.3	7.5	8.5		9.3	11	

3. Methods

Although the relative sea-level history along the Ionian coast of northern Calabria is acknowledged, an attempt to better decipher the number of orders, the physical continuity and the sedimentary significance of terraces, as well as the interplay of climatic and tectonic controls on terrace formation is needed. To this end, a key area was selected in a transect located between the Raganello and Coscile rivers (Figure 2) where many outcrops expose the terraced sequences. The aim of selecting a restricted area was to limit the tectonic effects of spatially variable uplift rates, largely invoked in the literature ([7] and references therein). Therefore, in order to reconstruct the stratigraphic setting and the Middle–Late Pleistocene evolution of terraced deposits, a multidisciplinary approach was used, involving sedimentological and the most traditional, reliable and fundamental principles of geomorphic analysis of the terraces.

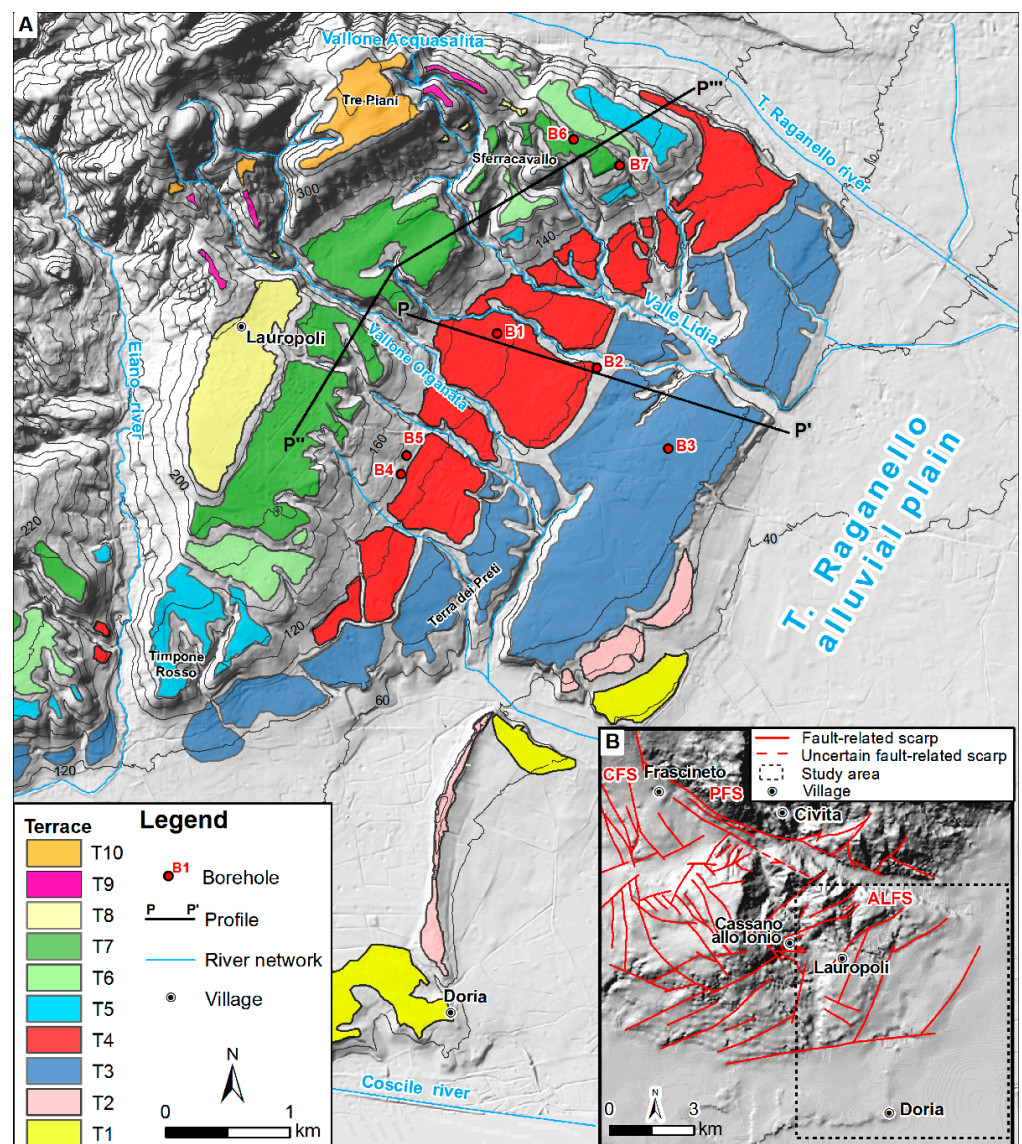


Figure 2. (A) Morphological map of the Middle–Late Pleistocene terraces between the Eiano and T. Raganello river valleys. Noteworthy are cross-cut relationships among terraces, well apparent on the right side of the T. Raganello. **(B)** Morphostructural map (modified after [5,27]); of the Ionian coast of northern Calabria. CFS: Castrovillari Fault System; PFS: Pollino Fault System; ALFS: Avena–Lauropoli Fault System.

The field surveys were performed with the aim of characterizing clastic sediment exposures and contact relationships, as well as identifying landscape features of different types and relative ages. Facies analysis was carried out in order to (i) point out specific assemblages of genetically associated facies (facies association) to be used for interpretation of the depositional environment; (ii) assess the presence of unconformities; and (iii) provide the meaning of the upper terrace surface. The sedimentary facies associations were distinguished by (i) lithology, grain-size, and sedimentary structures, (ii) stratal geometries and stacking patterns, and the (iii) fossil content.

A detailed geomorphological analysis of terrace remnants was performed through field surveys, aerial photo interpretation, and analysis of detail-scale topographic maps (1:10.000 and 1:5000 scale). The foregoing surveys were also key to the assessment of the elevation of the inner margin, particularly where it is covered by terrestrial sediments. Specifically, to assess the inner edge elevation of the terraces, we considered the uppermost position of foreshore deposits of the beach sequence. In Figure 2, the morphological knickpoint (and not the highest elevation of foreshore sediments) is mapped. Morphogenesis, relative chronology, altitudinal range, and morphological cross-cutting relationships were used as criteria to group the terraced landforms into different orders. Morpho-structural analysis in a sector wider than the study area was also carried out through aerophoto interpretation and 5 m DEM analysis for assessing fault-related scarps (*sensu* [28]; Figure 2B).

Additionally, to better characterize the terraced successions, well data from ISPRA [29] (<http://sgi2.isprambiente.it/indagini/> accessed on 12 January 2022) were analyzed.

4. Results

4.1. Facies Association

Four facies associations (FA) were recognized: FA1) fluvial and alluvial fan conglomerates and sandstones; FA2) beach or shallow-marine conglomerates and sandstones; FA3a) shoal-water delta sandstones and conglomerates, and FA3b) Gilbert-type conglomerates and sandstones. The description of sedimentologic and stratigraphic features of each FA is followed by their interpretations.

4.1.1. Fluvial and Alluvial Fan Conglomerates (FA1)

This facies association is mostly composed of horizontally bedded to crudely stratified conglomerates and intervening sandstones that locally rest on alternating sandstones, siltstone, and pebbly conglomerates. Specifically, three facies assemblages were recognized.

Facies assemblage 1 is made of laterally extensive siltstone and sandstone beds with intervening beds and lenses of granule- to pebble conglomerates that occur in ribbon-like bodies extending laterally for meters. Well-developed sedimentary structures are generally lacking, but parallel to low-angle cross lamination occurs. Locally, some siltstone and sandstone beds show rare rootlets and extensively developed carbonate-rich, soft-cemented horizons. Facies assemblage 1 passes rapidly upward by alternating to facies assemblage 2 composed of clast-supported, sheet-like, and crudely stratified conglomerates of pebble- to cobble-grade with clear overprinting of pedogenetic processes (Figure 3A). Beds are ungraded or normally graded with an overall tabular geometry. Basal bedding contacts are sharp and slightly irregular, with low-relief scour surfaces well developed on fine grained sediments consisting of crude, plane-parallel stratified sandstones and pebbly sandstone lenses, up to 0.30 m thick, reddish or brownish in color.



Figure 3. Overview of deposits and facies outcropping in the study area. (A) Clast-supported, sheet-like, and crudely stratified fluvial conglomerates (FA1; terrace T10). (B) Meter-thick topset unit resting erosively on the underlying foreset unit with oblique geometry (FA3b; terrace T6). (C,D) Sections normal

to the paleo-shoreline (land on the right) of the progradational beach sequence of terrace T3. At the transition between the upper and the lower beachface (C), the beds thicken and are characterized by more irregular stratification; the dip angle of gravel beds gradually increases down-dip where they interfinger with sand tongues and beds (close up view in C) interpreted as bar deposits migrating in the post-storm stage. Solid arrows indicate cross-bedding in the upper-beachface gravels forming lenticular units with erosional truncations at the top, interpreted as berm stratification (close up view in D). (E) The basal part of the succession consists of mouth-bar deltaic gravels forming broadly lenticular cross-beds stepping seaward. They are unconformably overlain (dashed lines) by upper beachface gravels (terrace T4). (F) Fluvial conglomerates resting erosively (white dashed line) on delta front sandstone beds that grade landward into mouth bar deposits (terrace T7). Overview (G) and detail (H) of gravelly and sandy foreset deposits interpreted as the sedimentary record of foreset beds of a Gilbert-type delta outcropping on the valley sides of Vallone Organata (terraces T9 and T10). White ellipse in Figure 3A,E marks the hammer for scale.

Locally, conglomerates form fining upward, meter-thick gravel units separated by undulating, erosional surfaces, and reddish paleosols (facies assemblage 3, Figure 3B). The gravel units commonly comprise a basal part constituted of very poorly to moderately sorted, clast-supported, pebbly, cobbly, fine boulder gravels overlain by horizontally, planar and crudely stratified, pebble-to fine cobble-conglomerate and laminated sandstone. The base of gravel units has a sharp, irregularly scoured geometry; pronounced scour-fills with up to 50 cm relief and characterized by U- or V-shaped cross-sectional geometry occasionally occur.

This FA1 is composed of aggradational units and is primarily interpreted as the result of terrestrial sedimentation in gravel bed rivers characterized by variable sedimentary pulses [30,31].

Specifically, facies Assemblage 1 suggests fluctuating energy, water-rich flows reflecting succeeding overbank flooding and minor channel formation (ribbon conglomerates) in a sheltered, lateral part of the floodplain or in interchannel zones, sometimes reached by major floods [30,31].

Facies assemblage 2 is considered the expression of braided-fluvial systems where the laterally extensive conglomerate beds represent migrating and accreting low-relief bars in high energy gravel bed rivers. The intervening sandstones, as well as minor scour-fill conglomerates, represent deposition from heavily sediment-laden flows during waning floods and/or minor channels cutting across bar tops and/or channel bend fronts during falling flood stages [32,33].

Facies assemblage 3 is interpreted as the result of low-relief, incised-channel deposition by high-magnitude flood-flows onto which a finer sediment deposition takes place through aggradation and/or lateral accretion during falling flood stages and/or during low-energy flows [32,34]. Cut-and-fill structures, characterized by pronounced erosional base, are interpreted as the filling of scours dissecting and remolding the top of in-channel deposits due to minor overland flows [35,36]. Stratal geometries and stacking patterns, along with fairly sloping and south-westward-facing consecutive convex surfaces, reveal a depositional slope formed by coalescent fan systems. In this regard, the superimposed fining-upward units could be attributed to the fillings of fan distributary channels dissecting fan surfaces.

4.1.2. Shallow-Marine Conglomerates and Sandstones (FA2)

Clinostratified conglomerate and sandstone layers are the dominant features of this facies association that crops out throughout the study area. Clinofolds show offlapping and downlapping internal pattern indicative of progradation and truncated by erosion surface in many places. In the studied successions, a lower part, lithologically heterogeneous, is distinguished from an upper part primarily consisting of clinostratified gravel deposits. Locally, shallow-marine successions show clear evidence of retrogradational to progradational stratal stacking patterns.

- Beachface conglomerates

Clinostratified gravel bodies, up to 12 m in thickness, consist of a lower and upper part showing different textural features, stratification types, and average dip angles of beds. The upper part of clinostratified gravel bodies is characterized by distinct, even, and thin

stratification with good clast-size segregation into high sorting, different beds consisting of granule- to medium pebble-sized clasts. At times, beds show vertical variations in clast sorting size and are composed of bimodally sorted, rounded pebbles. Gravel layers are planar to gently convex in the direction of progradation, with an average southerly inclination of 4° that decrease upslope where they locally form lenticular units showing erosional truncations and northerly accretion (Figure 3C,D).

Downslope, the fine-grained gravel beds wedge out and interfinger with pebble- to cobble-grade gravel layers characterized by crude, poorly distinct stratification (Figure 3C). Locally, lower boundaries are flat and sharp, showing southerly dipping erosional surfaces. The average bed inclination is $\sim 11^\circ$ and gradually increases downslope. Beds tend to wedge out clearly downslope, are primarily sigmoidal in shape, and tend to form juxtaposed gravel wedges separated by erosion surface.

The deposits forming the foregoing clinostratified gravel bodies of FA 2 represent beachface sediments of the reflective shoreline [37–39]. Specifically, thin, regular, and parallel stratification with good clast-size sorting is interpreted as the result of swash and backwash processes in the upper beachface. Layer bundles forming convex-up lenticular units (Figure 3C,D) represent deposition of higher berms characterized by landward accretion. Downslope, the beds of the upper beachface wedge out and interfinger with lower-beachface deposits, characterized by crude, poorly distinct stratification (Figure 3C). At times, at the transition to the upper beachface, the beds wedge out, sometimes showing erosional surfaces due to storm planation.

- Shoreface conglomerates and sandstones

Larger exposures, normal to the foregoing clinofolds, show distinctly sand tongues (Figure 3C) or gravel–sand couplets that wedge out at the toe of the beachface. Specifically, sand tongues climb up the lower beachface beds to some extent and show primarily onshore dipping planar stratified sand. Gravel layers show a very broadly lenticular geometry and are cm to dm thick. Clasts are in the pebble-cobble size range and display a poor preferred fabric; locally they are scattered or segregated into flat stringers/lenses. The sand layers and tongues interfingering with gravel beds tend to wedge out landwards and show basically onshore dipping planar stratification and subordinate through cross-stratification. Gravel–sand couplets grade downdip and alternate to intertangling sand and fine-grained gravels. Bedsets of subhorizontal to low-angle cross-stratified sand are bounded by sharp and broad shallow scours floored by gravels, pebbly-sands with small-sized mollusks remains. Amalgamated hummocky cross-stratified and flat laminated sands occur as rare interbeds up to 1 m thick and pass laterally (to the west) into crudely laminated sandy silts.

The typical interfingering of layers of sand and gravel along with the overall tendency of gravel–sand couplets to wedge out landwards and the toe of the beachface indicate storm and post-storm sedimentary record in the upper shoreface. Specifically, gravel beds result from the severe erosion of the beachface deposits, whereas onshore-dipping, cross-stratified sands are interpreted as the landward and/or longshore migration of the bar system during the declining stage of the storm. Gravel layers flooring low-relief erosion surfaces overlaid by horizontally to low-angle cross-laminated sands are interpreted as representing the record of the lower shoreface where migrating rip currents associate with low-amplitude nearshore bars during storms [37,40].

4.1.3. Deltaic Sediments (FA3)

The genetic relationships between the facies described below, the stratal geometry, and contact relationships of the facies assemblages indicate that deltaic deposits have both shoal-water or mouth-bar type geometry (FA3a) and Gilbert-type geometry (FA3b).

- Shoal-water delta conglomerates and sandstones (FA3a)

In completely developed sequences, the proximal part is constituted of a poorly sorted, clast- to sandy matrix-supported conglomerate of pebble to boulder grade alternating to massive and stratified sandstones. Conglomerates occur as lenticular and subordinate tabular bodies, commonly stacked in m-thick units characterized by concave up scour surfaces. Although the fabric is disorganized, they show irregular clusters of cobble- to

boulder-sized clasts and locally show weak grading. The disorganized gravel passes laterally and alternates to poorly to moderately sorted, clast- to sandy matrix-supported gravel of pebble to cobble grade, showing tangential to sigmoidal planar cross-stratification, up 8 m thick. The bedsets are 0.5–2 m thick and are separated by planar or undulating, erosive bases. The cross-sets are arranged in laterally offset stacking patterns (Figure 3E) with planar to erosional, concave-upward boundaries and appear to have filled dm-deep and m-wide scours in flow-transverse sections. Rare convex-upward gravel lenses are embedded. Cross-beds alternate downdip with horizontally and planar to trough cross-laminated sand and pebbly sand forming repeated cm- to dm-thick, fining-upward packages composed of horizontally and cross-stratified sand, with local basal gravel sheets and lenses, grading upward into ripple cross-laminated sandstone and silty mudstone. Basal contacts are usually sharp, planar, and locally erosive. Some beds contain large pebbles as subhorizontal trains, but lenticular gravel layers with pronounced concave-up erosional bases also occur. Commonly, thin horizontal and discontinuous pebbly layers composed of fine pebbles and granules are present. Further downslope (on the left side of Torrente Organata), they pass to poorly to moderately sorted, fine- to medium-grained sandstones (Figure 3F), with intervening fossiliferous silty mudstone and granular to fine-pebble conglomerate beds. Sandy deposits mainly consist of massive sandstone strata with sharp, non-erosive basal surfaces and tabular geometry.

Stratal features and lateral relationships of deposits indicate a stacked seaward-stepping architecture. In particular, the dominance of conglomeratic deposits and the downflow transition into finer-grained deposits suggest a record of proximal (mouth bar) to distal (delta front) sectors of a SE-prograding, fluvial-influenced, low-sloping shoal water delta system [41].

Specifically, the disorganized gravel deposits, the lack of internal stratification, and the non-preferred clast orientations suggest a mass flow origin for the sediments; they are found commonly in the proximal part of gravel units alternating with cross-stratified conglomerates interpreted as the deposits of stream-dominated floods. As a whole, their interbedding may be the expression of mouth bar-like bedforms characterized by downstream accreting cross-stratified bars due to composite sediment-laden stream flow [42,43]. They may be the result of (i) the rapid shifting of the channel mouth and associated sedimentary processes and (ii) the variation related to fluctuating flood levels with variable discharge and sediment concentrations. In particular cross-bedded gravels are thought to be formed at the mouths of delta-slope chutes and are attributed to scour-fills recording rapid cut-and-fill processes under varying flow [43,44].

The origin of the fining-upward bundles may be attributed to highly concentrated, fluctuating tractive currents in the proximal part of a delta front [45,46]. In particular, the gravel sheets and lenses, the flat-stratified sand, and the presence of low-angle curved erosion surfaces suggest highly sediment-laden, fluctuating turbulent flows with repeated scour and fill processes. Subsequent low flowstage conditions are suggested by ripple cross-lamination and silty mud drapes [44].

The fine- to medium-grained sandstone packages, with intervening fossiliferous silty mudstone and fine-grained conglomerate beds, are therefore interpreted as the product of highly sediment-laden fluvial floods that conveyed large volumes of sediments farther seaward, forming delta front sandstone lobes [47].

- Gilbert-type delta (FA3b)

The data derived from the facies analysis and stratigraphic architecture suggest the presence of two main stratal units of foreset and topset that are the result of the Gilbert-type braided delta sedimentation [20,48,49].

Clinostratified conglomerates and subordinate sandstones are the dominant features of the foreset facies assemblage. The gravels occur in steeply-inclined (N110°–180°) beds, having a broad sheet-like geometry and forming clinostratified sequences up to 30 m thick. The clasts range in size from granule to cobble and are either matrix- or clast-supported in a sand matrix. Minor changes in bedding inclination and dip direction are mostly coupled with internal truncations leading to the development of a concave-up dome and a mound-shaped lobate geometry. Indeed, meters wide, 0.4-m-deep bedsets locally form lens-shaped units consisting of stratified sand and granule to pebble-sized gravel (Figure 3G,H).

Apparent scour-based sets of upslope-dipping cross-strata up to 0.5 m thick occasionally occur. To the south–southeast, a progressive decrease in the bedding dip angle up to 8° and a higher sand/gravel ratio are well apparent. Shell fragments of bivalves sparsely occur.

A sharp and erosional surface marks at times the transition to the topset unit, up to 25 m thick. It consists of horizontally to subhorizontally, sheet-like, clast-supported gravel beds with scant, cm- to dm-thick sandy lenses. These beds, up to 1 m thick and meters wide, are locally truncated by scour surfaces, thus forming lens-shaped units. Clasts are pebble to cobble-grade, with subordinate boulders, and are mostly sub-rounded to rounded. Fine- and coarse-grained deposits are occasionally characterized by a reddish color, a clear sign of pedogenesis and subaerial exposure.

The stacking pattern of clinostratified bodies indicates a seaward prograding clastic wedge of a foreset unit of a Gilbert-type delta where deposition occur along a subaqueous slope through sediment gravity flows triggered by gravity and river floods [49,50]. Changes in the foreset dip angle may be interpreted as the product of variable aggradation/progradation rates [51], whereas minor scour-fills structures can be related to sudden changes in the velocity of low-density flow generating backset beds [52]. The topset unit represents the sedimentary record of migrating and accreting low-relief bars in a river braidplain [30,31], having many similarities with fluvial facies association, specifically to facies assemblage 2.

4.2. Geomorphological Data

The study area is characterized by terracing processes developed on the Early Pleistocene Lauropoli Conglomerates [21]. The south-eastern slope gently dips towards the Ionian coast, and its profile is interrupted by a ten-order stair of raised marine terraces (Figures 2 and 4), stepping between 350 and 40 m a.s.l, mostly of depositional origin, described in the following from the highest (T10) to the lowest (T1).

4.2.1. Terrace T10

Terrace T10 is differently developed in the study area. To the north, this terrace consists of a gently rolling isolated surface that rises up to 350 m, exceeds 800 m in width, and hangs on the T. Raganello River valley (Tre Piani surface; Figure 2). Small and discontinuous exposures, covering the Tre Piani surface, indicate the presence of fluvial deposits that rest unconformably on south-east facing bedsets; stratal features and lateral relationships indicate a progradational clastic wedge representing the sedimentary record of a Gilbert-type delta.

Southwest of the Tre Piani surface, the inner T10 margin elevation is detected through small-sized remnants hanging on the Vallone Organata. Footslope cross-profiles appear concave, with a low incline and characterized by thin alluvial cover or consist of erosional surfaces cutting the sandy and clayey deposits of the Lauropoli Formation.

Therefore, based only on morphologic correlations, the inner margin of T10 lies at elevations between 340 and 350 m, with the highest value in the northern part of the terrace.

4.2.2. Terrace T9

Crosscutting relationships among low-relief surfaces and the Tre Piani surface (T10 terrace) allowed us to detect small-sized remnants of terrace T9, locally reduced to narrow ridge-tops by strong dissection (Figures 2 and 4). West of the Vallone Organata, the terrace deposit consists of alluvial sediments resting erosively on the Lauropoli Formation. To the east, alluvial deposits rest unconformably on conglomerates and sandstone foreset beds forming the typical geometry of a Gilbert-type delta (FA3b).

Despite the large inaccuracy in the correlation, the width, slope, and elevation range of concave-up, footslope cross-profiles have been used to assess the morphological inner margin elevation of the T9 terrace between 290 and 310 m.

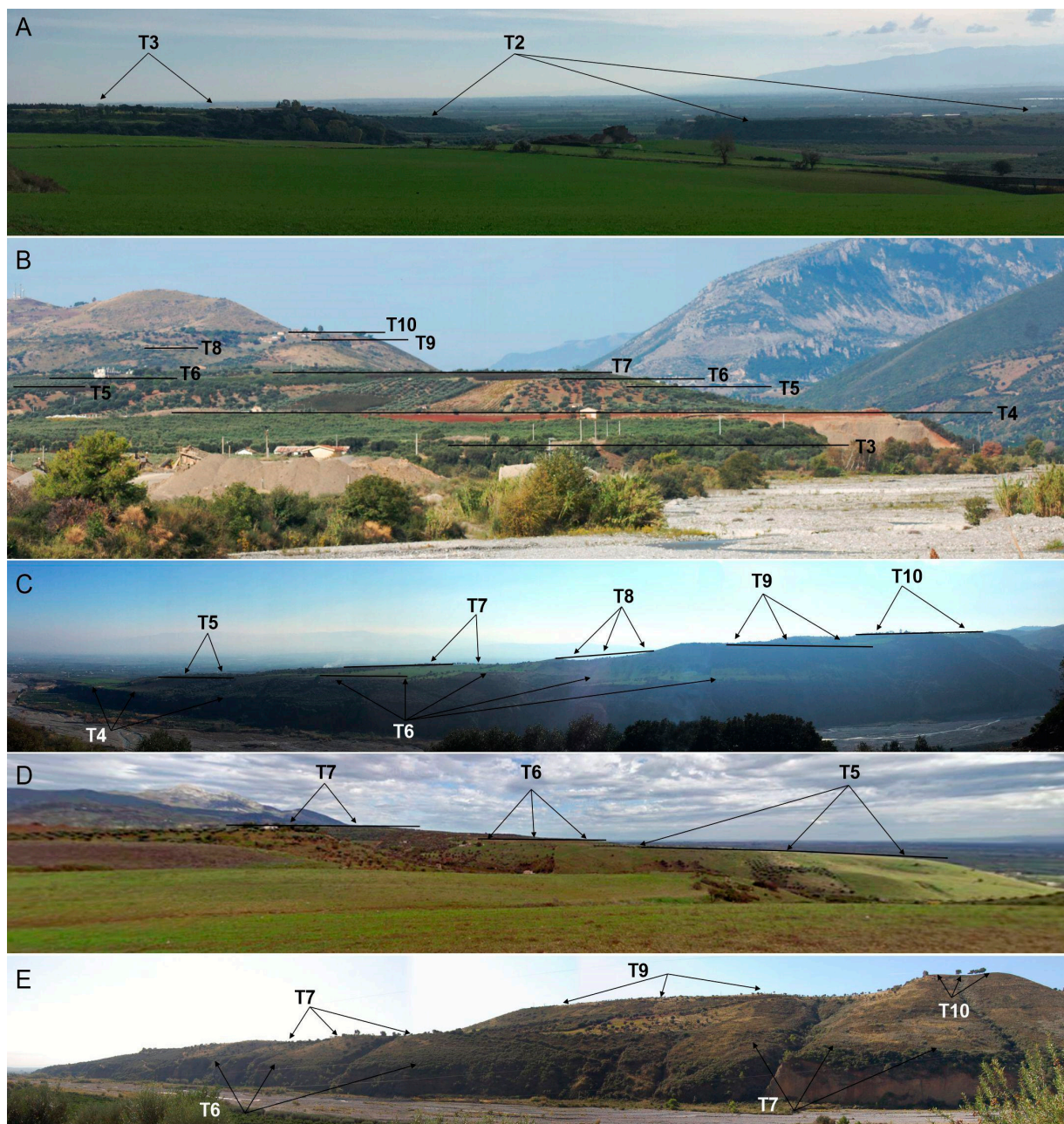


Figure 4. Overview of landscapes in the study area; arrows indicate terrace order. (A) View from the west of the Doria ridge inset into terrace T3. (B,C) The T. Raganello river valley shows amazing views of most of the stepped flight of terraces; it is worthy to note the telescopical arrangement of terraces. (D) View from the west (Timpone Rosso) of the terrace flights on the left side of the Eiano river. (E) Overview of the oldest terraces (T6–T10) characterized by clear cross-cut relationships on the right side of the T. Raganello river.

4.2.3. Terraces T8–T5

At elevations between ~250 m and 140 m, an extensive gently rolling landscape rises up. Such a morphologic feature has been ascribed to terrace T3 by [4], T6 by [6], and T5 by [7]. In fact, the above-described landscape consists of several land surfaces (up to ~900 m in width), regularly distributed over the study area (Figures 2 and 4). In particular, by analyzing in detail 1:10.000 and 1:5.000 topographic maps, such surfaces show clear cross-cut relationships among themselves (Figure 2). Southeast of Lauropoli, an increase in the slope gradient at elevations between 225 and 215 m is noteworthy. On the right side of

the Raganello River valley, the inner edge elevation of the highest terrace (terrace T8) is represented by the concave-up knickpoint between 235 and 245 m (Figure 2), whereas the outer margin is at an elevation of ~225 m. Exposures along the terrace edges concern only the uppermost part of the successions composed of fluvial deposits.

Close to the northeast of Lauropoli, a lower terrace (terrace T7) is noticeable. The inner edge elevation has been assessed through the uppermost elevation of the foreshore deposits between 210 and 215 m, whereas its outer margin is at an elevation of ~195 m. In the southwestern part of Lauropoli, artificial exposures allow us to assess a fluvial succession of about 10 m in thickness consisting of conglomerates of FA1 (facies assemblage 2). Along the valley sides of the Vallone Organata, the terrace deposit is primarily composed of gravelly and sandy mouth-bar deposits of FA3a onto which fluvial conglomerates of FA1 (facies assemblage 2) rest erosively. Along the left side of the Vallone Organata, close to the outer terrace margin, it is worth noting that fluvial deposits are encased and rest erosively on delta front sediments of FA3a (Figure 3F). Instead, to the northeast, the terrace deposit consists of foreset and topset beds of a Gilbert-type delta (FA3b).

Downslope of the terrace T7, cross-cut relationships (Figures 2 and 4D) allow us to detect two other surfaces, well south of Lauropoli. Their morphological inner margins are represented by knickpoints between 185 and 195 m (terrace T6) and at elevations of ~175 m (terrace T5). These terraces consist of apparent landsurfaces that hang on the left side of the Eiano River valley and are up ~700 m in width (Figures 2 and 4D). Many small exposures along natural and artificial scarps indicate an overall stratal architecture indicative of a progradational gravel beach sequence, which allow us to assess the inner margin elevation at ~190 and ~175 m for terraces T6 and T5, respectively.

To the northwest, near the T. Raganello River valley, the aforementioned cross-cut relationships are less apparent because of thick alluvial covers of the upper part of the terraces. Specifically, based on bed geometry and bedset stacking, the two terraces are telescopically inset within each other, producing a suite of downward-diverging terrace surfaces consisting of forward-stepping of Gilbert-type deltas (FA3a).

4.2.4. Terrace T4

In the study area, terrace T4 remnants are fairly homogeneous in size, with a mean width of 1000 m and a slope value of about 2° (Figure 4B). Based on morphological features, the inner margin of T4 lies at elevations spanning from ~145 to ~130 m, with the highest values found in the northern part of the study area. The uppermost elevation of the foreshore deposits is at ~115 m. The lateral and in-valley continuity of the terrace is very apparent close to the T. Raganello River (Figure 2) where excellent quarry exposures occur. Here, the terrace deposit has a thickness of ~25 m and is composed of Gilbert-type delta deposits that grade basinward (to the SE) into mouth-bar conglomerates and sandstone passing upward into beachface gravels (FA2). The clastic succession ends with fluvial deposits (FA1, facies assemblage 2) whose basal contacts are usually sharp, planar, and locally faintly erosive; it is worth noting is that facies assemblage 2 grades progressively to facies assemblage 3 moving southwestwards where the quite continuous, fairly sloping, and south-westward facing surface of terrace T4 reveals a depositional slope formed by coalescent fan systems.

4.2.5. Terrace T3

Terrace T3 is well preserved south of the T. Raganello River (Figure 4A,B). Its inner margin is traced at an elevation ranging between ~90 m along the Valle Lidia and ~100 m at the Terra dei Preti sites, where the terrace width exceeds 1500 m (Figure 2). The gravel beach sequence (FA2) associated to the terrace is widespread over the area, with thickness exceeding 20 m. Field evidence from the many exposures along the lower reach of the Vallone Organata indicates that the terrace succession is characterized by a transgressive-regressive cycle. Further, it is worth noting the occurrence of synsedimentary extensional

faulting affecting beach sediments. In the area of Valle Lidia, beach deposits pass laterally to fluvial conglomerates of facies assemblage 1 of FA1.

4.2.6. Terrace T2–T1

North of Doria village, terrace T2 consists of a narrow, isolated ridge, juxtaposing to terrace T3 to the northeast (Figures 2 and 4A), with which it shares the architecture style. Based on the uppermost elevation of foreshore deposits, along with morphological correlations, the inner margin of T2 is at an elevation of ~65 m. The Doria ridge can be further correlated with a terraced surface hanging on the left side of the Coscile river at elevations between ~65 and ~75 m (Figure 2), where the terraced deposits consist of fluvial deposits.

Morphological evidence indicates clear cross-cutting relationships between the Doria ridge and a lower flat-lying surface that lies at elevation ranging from ~40 m to ~50 m south and northwest of the Doria ridge, respectively. This surface, named T1, has no evidence of marine origin. Indeed, even though small and discontinuous, the presence of many natural and artificial exposures along the left side of the Coscile River indicate the presence of fluvial deposits of Facies assemblage 1.

5. Discussion

5.1. Terrace Chronological Correlations

A ten-order stair of raised terraces, stepping between 350 and 40 m a.s.l., represents the main geomorphological feature of the area (Figure 2). The terraces are mainly of depositional origin with the oldest primarily constituted by fluvial–deltaic coastal plain deposits, whereas the youngest by beach sequences.

Although the elevation of the MIS 5.5 (124 ky) is typically considered the key marker for terrace flights' chronological constraints in the Mediterranean region, its definitive identification in the study area is still lacking (Table 1). Northward of the study area, a terrace lying between 102 and 115 m in elevation was attributed to the MIS 5.5 based on radiometric analysis [53,54] and was correlated with the T4 terrace of [4] standing at ~110–130 m (Table 1). To the north and south of the study area, Santoro et al. (2009) attributed the terrace standing at 94–112 m in elevation to the MIS 5.5. This terrace was later included in the 120–125 m terrace by Santoro et al. (2013) and assigned to the same MIS 5.5.

In this work, sedimentary facies analysis, mapping of foreshore deposits, cross-cut relationships between terraced surfaces, and morphological observations allowed us to split the MIS 5.5 terrace of [4,7] into two terraces with inner edges standing at ~90–100 m (T3 terrace) and ~115–120 m (T4 terrace). This hypothesis is supported by field and borehole data. Indeed, close to the morphological inner-edge of T4, a 20-m-thick clastic wedge succession decreases in thickness and appears to taper on clay sediments to the east (Figure 5A). Although borehole data do not provide any indication on the conglomerates underlying 8-m-thick alluvial fan facies, the whole conglomerate succession rests on a presumably erosion surface, developed on clayey substratum currently at about 100 m a.s.l. Further to the west, the contact between conglomerates and clayey sediments is at about 65 m a.s.l. Here, a transgressive–regressive sequence of the gravelly and sandy beach of the T3 terrace shows an apparent onlapping stratal geometry and rests erosively on the underlying clayey sediments, with a gently inclined lower bounding surface (Figure 5A).

Therefore, based on age constraints provided by [4,6] and on the average regional uplift of ~1 mm/y since the Last Interglacial [1,2], the T4 terrace mapped in this study between ~115 and 120 m (the highest elevation of foreshore sediments) is correlated with the Marine Isotopic Stage (MIS) 5.5, aged at ~124 ky. Using the inferred uplift rate of ~1 mm/y deduced from the elevation of the MIS 5.5, we indirectly correlated other marine terraces in the investigated area to sea-level stands (Figure 6). Although there is no complete agreement among the many relative sea level curves published in the literature [55], we correlated the corresponding inner T4 edges with many sea-level stands of the sea level

curve, as previously applied in the Ionian sector of northern Calabria [5–7,9,10]. Although the expected terrace elevation does not always well match the present-day altitude of the observed inner margins, by applying a constant uplift rate evaluated from T4 inner margin elevation, we obtained the following correlations for the upper terraces (Table 1, Figure 6): T5 to MIS 7.1, T6 to MIS 7.3, T7 to MIS 7.5, T8 to MIS 8.5, and T9 to MIS 9.3. For the highest terrace (T10), we found that the best correlation age was with MIS 11.

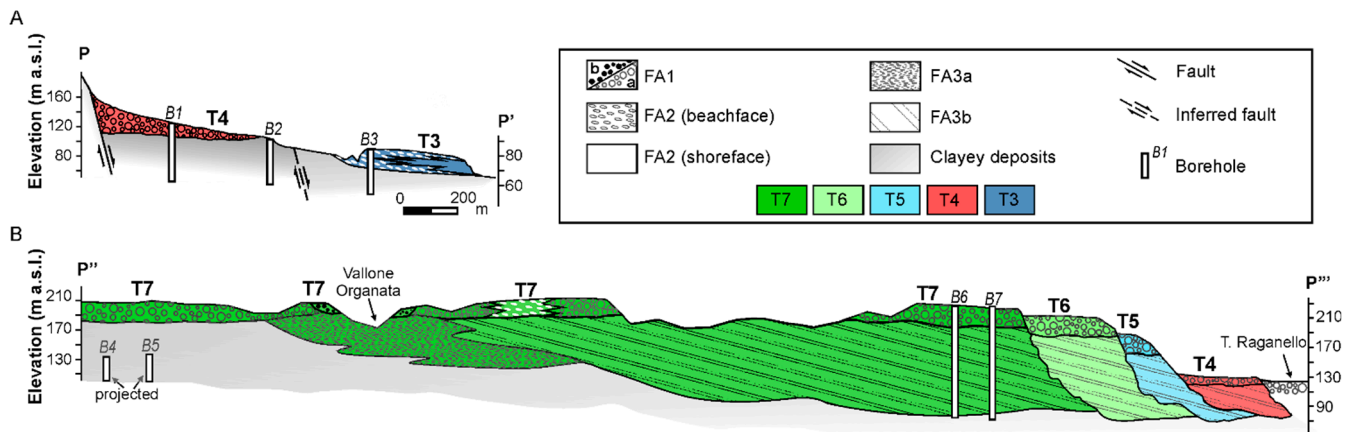


Figure 5. Morphostratigraphic sections showing the relationships among the clastic successions of terraces. (A) View of T4 and T3, on the left side of Vallone Organata. Alluvial conglomerates show an eastward decrease in thickness and taper on clayey sediments near the outer T4 edge. A clastic transgressive–regressive sequence is noteworthy on the T3 terrace. (B) Lateral and vertical variations in facies association are well noticeable on the T7 terrace where Gilbert-deposits (FA3b) pass laterally to shoal-water delta sediments (FA3a) and are overlain by fluvial conglomerates and locally by shallow marine deposits. For each FA, the color refers to different orders of terraced deposits. See Figure 2 for profile and borehole location.

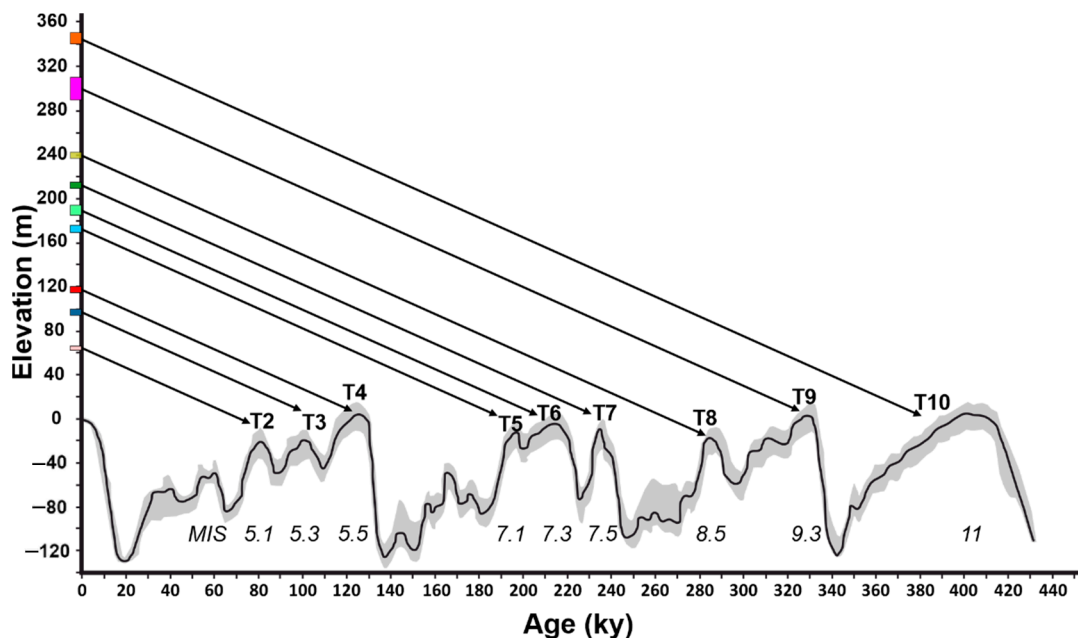


Figure 6. Chronological correlations between observed marine terraces and sea level peaks of the [56] sea level curve (bold black line). The light grey area marks the associated confidence interval. Numbers in italics indicate the marine isotopic stage (MIS). The colored rectangles along the ordinate axis point at the present day elevation range of the inner edges of different terrace orders (the colors are the same as in Figure 2). The solid arrow marks the expected chronological correlation, based on an average uplift rate of 1 mm/y.

The resulting chronological scheme (Table 1) for the whole flight mainly differs from literature data [4–7] insofar as the authors described a single terrace in the study area, with an inner margin elevation between 220 and 240 m above the MIS 5.5, compared to the four terraces (T5–T8) distinguished in this work. The four T5–T8 terraces conceivably mark many sea-level stands older than 124 ky (MIS 5.5), below which we describe three terraces differently from previous works. Their altitude distribution is very apparent from cross-cut relationships between the terraced surfaces and the related deposits. For terraces T2 and T3, we found that the best correlation was with MIS 5.1 and 5.3, respectively. Given the inferred uplift rate of ~1 mm/y, the poor fit between the terrace T3 elevation with the MIS 5.3 can be accounted for by an increase in uplift during the MIS 5 (e.g., [6]). The lack of beach deposit outcropping on terrace T1 makes it difficult to correlate the lowest terrace mapped in the study area with any MIS.

5.2. Stratigraphic Architecture of Terrace Deposits

Based on the genetic relationships between the facies described in this paper, deposition occurred in a range of clastic environments associated with alluvial, deltaic, and beach depositional systems. In particular, the conglomerates and sandstones were deposited largely from different sedimentary processes acting on the mouth-bar/delta-front slope (FA3), passing laterally and upward to beach sediments (FA2). Alluvial sediments (FA1) were sourced by shallow gravel-bed braided streams and, locally, by coalescent alluvial fan systems in a similar way to present drainage in the study area. Observations of the contact relationships at several key localities show that the above facies associations, although characterized by lateral variations, are juxtaposed by scarps, locally fault-controlled (Figure 2B), and allow cross-sections across various parts of the terraced successions to be assembled.

Most of the terraced successions (from T4 to T10) show only their upper parts, characterized by shoaling upwards from delta (FA3) to beach deposits (FA2) and fluvial/alluvial facies association (FA1) (Figure 5B). In the northeastern sector, steeply inclined fore-set conglomerates (FA3b) mostly characterize the terraced successions from T4 to T10 (Figure 3G,H), which onlap onto the bedrock with alluvial, fluvial or shallow marine facies. To the west-southwest, alluvial conglomerates (FA1) extensively occur and locally abruptly overlie the well-sorted, planar- to cross-bedded sandstones and conglomerate of FA2 as well as the sediments of FA3a sandstones and conglomerates (Figures 3F and 5B) that are laterally equivalent to FA3b. Locally, alluvial conglomerates form thin patches of sediments where small-sized remnants of terraces are reduced to narrow ridge-tops by strong dissection and correlate with concave-up, low-inclined footslope cross-profiles characterized by thin alluvial/colluvial cover resting erosively on the sandy and clayey deposits of the Lauropoli Formation (T8 and T9 terraces). To the southwest (west of the Vallone Organata), erosive based alluvial facies (FA1) rest directly on the Lauropoli Formation (T8 terrace) or appear to erosively overlie shelfal, clayey deposits passing laterally to deltaic sediments (T7 terrace; Figure 5B).

Only for the T2 and T3 terraces, away from the main drainage lines, did most of the sedimentary successions crop out. The basal part of the terraced successions is apparent and interpreted as a flooding surface. Indeed, the sedimentary succession is characterized by a basal retrogradational stratal-pattern trend indicating a marked backstepping of the beach depositional system and the progressive drowning of the clayey substratum through a vertical facies shift from the beachface to the shoreface (Figure 5A). The following basinward progradation is marked by facies shifting from deeper to shallower water facies. As a whole, the T2 and T3 terraces are characterized by a transgressive/regressive arrangement of progradational gravel beach sequences (FA2). Only close to the T. Raganello River did small exposures along the outer T3 terrace edge indicate a lateral, erosive transition between fluvial facies of FA1 and beach sediments.

In particular, the T4 and T7 terraces show the best exposures of the highest terraced successions, which allow us to better assess stratal geometry and lateral and vertical variations in facies association. In fact, along the right side of the Raganello, i.e., the telescopic

in-valley part of the T4 terrace river (Figure 4B,C), clear evidence of progradation and aggradation are correlated with a Gilbert-type delta system. Such deltaic deposits pass to the ESE to stacked beds of mouth bar-like bedforms overlain by conformably to erosive-based beachface deposits of FA2. The topmost horizontal strata of FA1 (Figure 7), i.e., braided fluvial sediments, grade laterally, to the southwest, into a coalescent alluvial fan system (Figure 5A). Instead, Gilbert-type delta deposits of the T7 terrace pass laterally to the southwest to shoal-water delta sediments (FA3a) overlain by widespread fluvial conglomerates that appear to rest erosively on clayey deposits further to the west (Figure 5B).

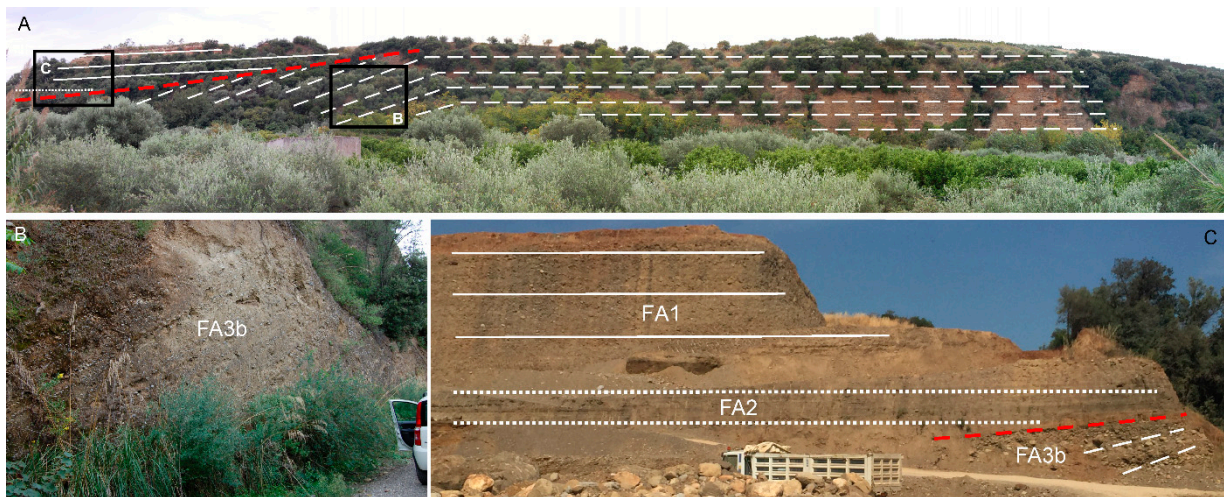


Figure 7. Overview (A) and details (B,C) of stratigraphic successions of the T4 terrace. Gilbert-delta (FA3b) conglomerates and sandstones (A,B) pass upward (red line) to beach sediments (FA2, dotted line) that are overlain (C) by fluvial deposits (FA1, solid line).

Facies transitions, commonly with evidence of stratigraphic discontinuities and morphological cross cutting relationships, suggest that the related depositional systems developed primarily in response to relative sea-level changes in conjunction with uplift. A possible scenario, inferred from vertical and lateral relationships of the facies associations of the T4 terrace, can be reasonably extended to the T4–T10 flight of terraces.

Stratigraphic architecture of the Gilbert-type delta of T4 terrace (Figure 7) shows clear evidence of delta aggradation to progradation (Figure 7A) followed by a basinward shifting of coastal facies associations (progradation to aggradation *sensu* [51]). In fact, mouth bar gravels tapering landward pass to progradational beach sediments (Figure 3E) and then to braided fluvial deposits (Figure 7B). Although such architecture can result from climatically driven fluctuations in sediment input and autocyclic delta-mouth shifting, we discard this hypothesis because (i) pollen records from southern Italy, specifically in mountainous areas close to the sea [57–59], indicate a persistent availability of moisture during both glacials and interglacials, which promoted an almost continuous sediment supply to the fluvial system and (ii) the uniform SSE dip of foreset strata reveals a constant sediment delivery. In addition, the presence of Gilbert-type and shoal-water geometries that developed in the same delta complex (T7 terrace, Figure 5B) may suggest an along-strike variation in fault-controlled subsidence and accommodation space, producing variable hanging wall relief over short distances.

Accordingly, during the relative sea-level fall and lowstand, an erosive surface is believed to originate from subaerial erosion, i.e., deep river erosion chiefly along the Raganello River valley, filled during relative sea-level rise by incised-valley systems [60,61]. Only for the T7 terrace is the first early phase of relative sea-level fall represented by erosive-based, fluvial conglomerates resting erosively on delta-slope deposits of FA3a (Figures 3F and 5B). Although the base of older terraced sequences (T4–T10) is not apparent in outcrops, the morphological cross-cutting relationships among the terraces (Figures 2 and 5B) suggest

the presence at the base of the terraced successions of concave-up erosion surfaces. In fact, terraces are noticeably telescopically inset within each other, producing a set of downward-diverging terrace surfaces (Figures 2 and 4; e.g., [9,10]).

The incised valley system was then flooded by the sea and formed a coastal embayment-like ria. Although most of the valleys are backfilled during the successive transgressive phase, deltas may develop at times when sediment supply exceeds the rate of relative sea-level rise [60,61]. Unfortunately, no evidence of in-valley transgressive marine deposits has been documented, but transgressive stages may be supported by the stratal geometry of Gilbert-type deltas. Indeed, the main valley fill is characterized by prograding coarse-grained, Gilbert-type delta deposits with evidence of aggradation to progradation (transgressive stages according to [51] followed by basinward progradation of deltaic to fluvial sedimentary systems during highstands (Figure 7). Due to sustained uplift rates, the resulting depositional surfaces become well entrenched within the previous uplifted and dissected landscape hanging from a few meters to some tens of meters above the more recent base level (Figures 4 and 5B).

Away from the incised-valley systems, borehole data (<http://sgi2.isprambiente.it/indagini/> accessed on 12 January 2022) suggest that the basal surface marking the subaerial erosion is directly overlain by transgressive shelfal deposits (Figure 5B). Next to the coastline, the transgressive beach deposits have not been recognized in outcrops, but boreholes (Figure 5A, T4 terrace) indicate a fairly horizontal, possible erosion surface cutting a clayey substratum underlying a conglomeratic clastic wedge that progressively thins to the SSE, at the outer edge. Further, the occurrence of non-marine conglomerates above marine strata suggests that the alluvial sedimentation was subsequently widespread across the area and not necessarily restricted to river outlets (coastal plain sediments).

5.3. Controls on Forward-Stepped Architecture

As stated above, repeated cycles of incised valley development (sea level fall) and aggrading to prograding deltaic and fluvial depositional systems (sea level rise and highstands) are responsible, along with uplift, for the forward-stepping terraced successions. Although the above-described architectures have similarities with the models proposed in the literature [51,62], our scheme differs insofar that it ascribes the morpho-stratigraphic evolution of the terraced successions to high-frequency, relative sea-level changes in the framework of sustained uplift, coupled with larger events of displacement.

Based on terrace extent (Figure 2) and elevation ranges (see Section 4.2), the studied terrace staircase may be partitioned into two terrace triplets (T10–T8 and T7–T5) and two terrace couplets (T4–T3; T2–T1) that are separated by scarps inducing a more marked spacing between each terrace group. Such scarps can be related to the Avena–Lauropoli fault-system [7,27], and therefore can be considered fault-related scarps that are systematically sealed by terraced deposits as the telescopic arrangement supports (Figure 4). We refer the forward-stepping of the terraced successions and the resulting downward-diverging terrace staircase to a general relative sea-level fall punctuated by short periods of sea-level rises, balanced by sediment supply in a framework of sustained uplift. This resulted in an overall time-inclined falling sea-level curve onto which short sea-level rises are superimposed (e.g., [51] and references therein). Hence, it is reasonable to assume that the spacing among each group of terraces is controlled by a local increase in uplift rates. It produced longer periods of relative sea-level falling stages, with higher amplitude of sea-level falls for MIS 8 and 6 (Figure 8).

Ref. [6] also argued that uplift was not constant during time and was characterized by the alternation of more rapid and slower periods of displacement. The authors claim that a higher uplift occurred during MIS 9 and 7 and the second half of MIS 5. Our findings indicate a more rapid uplift occurrence between MIS 8.5 and 7.5 and between MIS 7.1 and 5.5. In the light of the foregoing remarks, the ENE- to NE-striking morphological scarp bounding the outer T3 terrace edge, interpreted as a fault-related scarp, suggests a period of rapid uplift since MIS 5.3, slightly older than the one claimed by [6].

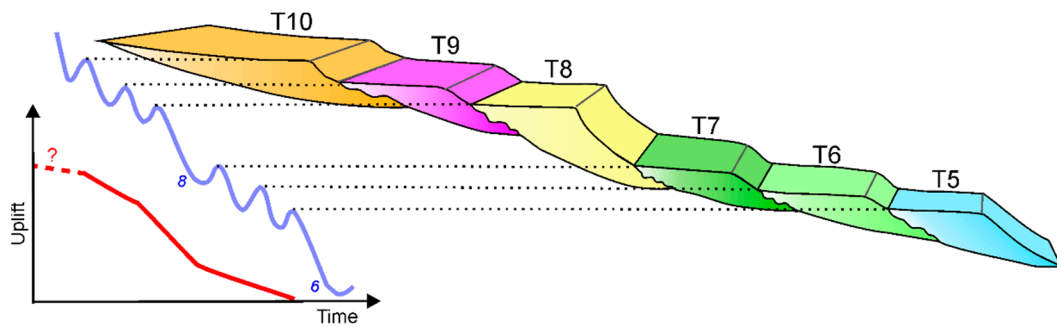


Figure 8. Sketch of terrace spacing resulting from the interaction between sea level curve (simplified blue line) and uplift variation over time (red line). Blue numbers in italics indicate marine isotopic stages. Terrace colors are the same as those in Figure 2. It is noteworthy that the figure is not to scale.

Further, vertical trends in the architecture of the deltaic succession (T7 terrace; Figure 5B) show different stratal stacking patterns related to variation in subsidence rates over time. In particular, the Gilbert-type delta passing westward to the shoal-water-type delta (Figure 5B) is interpreted as due to variations in accommodation space. Such an architecture may result from the activity of basin-bounding faults that may have induced along-strike variation in the hangingwall morphology (e.g., [48,63]). Although for T7 terraced successions there is no evidence of fault-induced along-strike variation in basin margin physiography, the E-trending normal faults affecting the T3 terrace produced a staircase geometry that well accounts for variations in subsidence rates towards the NE (Figure 9). Therefore, it is reasonable to assume that this fault-controlled subsidence affected the local thickening of terrace deposits and deepening of sedimentary environments (T3 terrace), affecting the lateral juxtaposition of different depositional systems (T10, T7, and T4 terraces).



Figure 9. T3 terrace shallow-marine conglomerates and sandstones (FA2). The contact between beachface gravels and shoreface sandstones and conglomerates is displaced by a synsedimentary NE-SW-trending normal fault responsible for the NE-directed increase in fault-controlled subsidence and thickening of terraced succession. B: Beachface; uSh: upper Shoreface; lSh: lower Shoreface.

In the Crati Valley, ref. [64] claimed that the Pleistocene Synthem of [65] deposited in a syn-rift wedge that thinned towards the Pollino Fault, promoting a favorable setting for the development over time of a Gilbert system. During Quaternary times, the Pleistocene Synthem was affected by tectonic fragmentation of the Pollino and Castrovillari Fault System (Figure 2B), connected through the Avena–Lauropoli NE-trending fault array [27].

Based on the above considerations, the Middle–Late Pleistocene morphostratigraphic evolution of the study area can be outlined: the very first evidence of the relationships between Gilbert-type delta systems and terracing processes is represented by the T10 terrace (Figure 10A), resulting from the interaction between eustatic sea level changes and tectonic uplift. The related sedimentary succession consists of a clastic wedge bounded to the East and to the West by the Pollino Fault and the Castrovillari Fault systems, respectively (Figure 2B), and its development was controlled by the Avena–Lauropoli fault system.

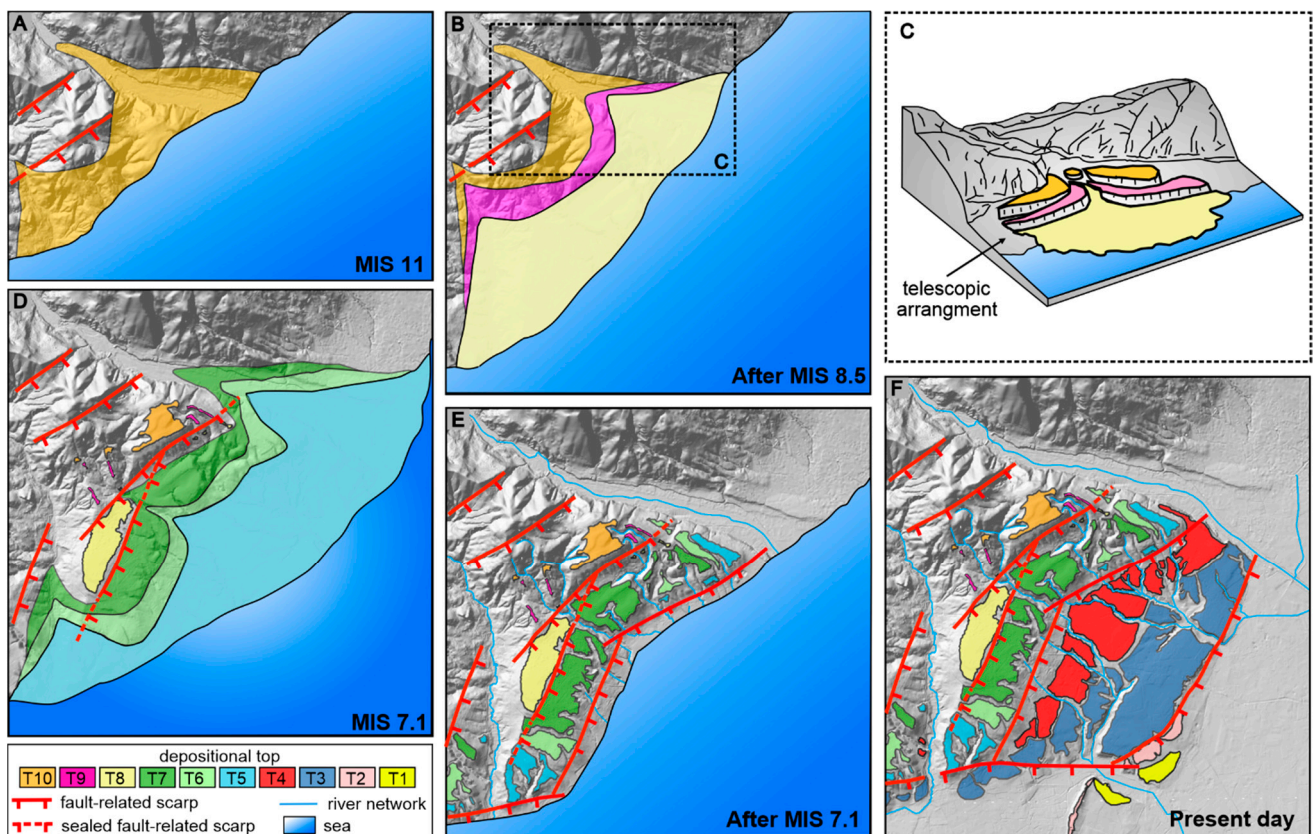


Figure 10. Morphotectonic evolution sketch of the study area. During MIS 11 (A), a Gilbert-type delta deposited (T10 terrace). Subsequent relative sea-level changes led to the development of two incised-valley systems (B), producing after MIS 8.5 a telescopic arrangement of T10–T8 terraces (C). Up to MIS 7.1, a new triplet of depositional bodies formed due to the interplay between uplift and sea-level curve (D). A NE-trending fault system changed the T7–T5 terrace triplet (E) and its basinward migration created the accommodation space for the younger depositional wedges which were terraced over time (F).

The following terraces (T9 and T8 terraces) sealed the NE-trending faults and are characterized by a forward stepping telescopic arrangement (Figure 10B,C), as a consequence of the time-inclined falling sea-level curve caused by sustained uplift (see Section 5.2).

The main fault-related scarps separating the T10–T8 and T7–T5 terrace groups (Figure 10D,E), inducing a marked spacing between them, consistent with a subsequent basinward migration of NE-trending faults that produced higher amplitudes of the relative sea-level falls (Figure 8). The above cyclicity modulated by fault migration lasted until the Late Pleistocene (Figure 10F). Based on chronological correlations (see Section 5.1), the time interval between the highest uplifts appears to shorten over time: ~150 ky between T10 and T8), ~100 ky between T7 and T5, and ~30 ky after the T3 terrace (Figures 6 and 10F).

Therefore, the morphostratigraphic evolution of the study area is linked to changes in uplift rates, eustatic sea-level fluctuations complemented by fault-controlled subsidence, and accommodation space induced by the Pollino and the Castrovillari Fault systems. Additionally, the SE-migration of the Avena–Laupoli Fault system is crucial for the development of the forward-stepping morpho-architectures of the terraced sedimentary successions.

6. Conclusions

A morpho-stratigraphical approach was used along the well-developed and preserved flight of the marine terrace that contours the northern Sibari Plain (northeastern Calabria). Cross-cut relationships in the terrace sequence, site-by-site sedimentological analyses

of the terraced deposits, and the revised chronological correlations provided valuable evidence about the morpho-sedimentary evolution and its relationship to sea-level changes and uplift.

Stratigraphic and sedimentologic analysis allowed us to distinguish a number of assemblages that were genetically associated (facies association). Lateral and vertical facies association changes allowed us to group them into different, superimposed, and juxtaposed depositional systems. As a whole, terraced sedimentary successions indicate an upward transition from marine and deltaic deposits to alluvial conglomerates as well as an ESE-directed progradation of the depositional systems.

Morphological cross-cut relationships among terraces, stratal architecture, and bounding surfaces allowed us to define a ten-order stair of raised marine terraces stepping between 350 and 40 m (a.s.l.). Specifically, analysis of the vertical and lateral stacking pattern of successions indicated repeated cycles of valley incision and alternating stages of coastal aggradation and progradation, attributed to high-frequency, relative sea-level changes, in the framework of sustained uplift resulting in a relative time-inclined falling sea-level curve.

Variations in local fault-induced subsidence and uplift rates also account for lateral changes in stratal geometries and stacking patterns and for the better spacing among groups of terraces. Further, the basinward migration of NE-trending faults was clearly featured by the telescopic arrangement of terraces that appears to seal the NE-striking fault traces over time, related to the main fault-related scarps separating groups of terraces.

Our morpho-stratigraphical approach to the studied flight of marine/coastal terraces contributed to providing new insights into the Middle–Late Pleistocene evolution of this key area of the southern Apennines, encouraging further analysis of geomorphological and stratigraphical data to better constrain the control of tectonics in shaping the morpho-stratigraphic architecture in the nearby coastal areas.

Author Contributions: Conceptualization, G.R.; investigation, A.B., F.L., G.R. and V.T.; data curation, F.L. and G.R.; visualization, F.L. and G.R.; writing—original draft preparation, F.L. and G.R.; writing—review and editing, F.L., G.R. and V.T.; supervision, F.L. and G.R. All authors have read and agreed to the published version of the manuscript.

Funding: This research received no external funding.

Data Availability Statement: All data obtained and analyzed during this study are available within the text.

Acknowledgments: The authors would like to thank two anonymous reviewers whose comments and suggestions improved the quality of the manuscript.

Conflicts of Interest: The authors declare no conflict of interest.

References

1. Bordoni, P.; Valensise, G. Deformation of the 125 ka marine terraces in Italy: Tectonic implications. In *Coastal Tectonics*; Stewart, I., Vita-Finzi, C., Eds.; Geological Society of London, Special Publication: London, UK, 1998; Volume 146, pp. 71–110. [\[CrossRef\]](#)
2. Ferranti, L.; Antonioli, F.; Mauz, B.; Amorosi, A.; Dai Pra, G.; Mastronuzzi, G.; Monaco, C.; Orrù, P.; Pappalardo, M.; Radtke, U.; et al. Markers of the last interglacial sea-level high stand along the coast of Italy: Tectonic implications. *Quat. Int.* **2006**, *145–146*, 30–54. [\[CrossRef\]](#)
3. Cucci, L.; Cinti, F.R. Regional uplift and local tectonic deformation recorded by the Quaternary marine terraces on the Ionian coast of northern Calabria (southern Italy). *Tectonophysics* **1998**, *292*, 67–83. [\[CrossRef\]](#)
4. Cucci, L. Raised marine terraces in the Northern Calabrian Arc (Southern Italy): A ~600 Kyr-long geological record of regional uplift. *Ann. Geophys.* **2004**, *47*, 1391–1406. [\[CrossRef\]](#)
5. Ferranti, L.; Santoro, E.; Mazzella, M.; Monaco, C.; Morelli, D. Active transpression in the northern Calabria Apennines, southern Italy. *Tectonophysics* **2009**, *476*, 226–251. [\[CrossRef\]](#)
6. Santoro, E.; Mazzella, M.; Ferranti, L.; Randisi, A.; Napolitano, E.; Rittner, S.; Radtke, U. Raised coastal terraces along the Ionian Sea coast of northern Calabria, Italy, suggest space and time variability of tectonic uplift rates. *Quat. Int.* **2009**, *206*, 78–101. [\[CrossRef\]](#)

7. Santoro, E.; Ferranti, L.; Burrato, P.; Mazzella, M.E.; Monaco, C. Deformed Pleistocene marine terraces along the Ionian Sea margin of southern Italy: Unveiling blind fault-related folds contribution to coastal uplift. *Tectonics* **2013**, *32*, 737–762. [[CrossRef](#)]
8. Caputo, R.; Bianca, M.; D’Onofrio, R. Ionian marine terraces of southern Italy: Insights into the Quaternary tectonic evolution of the area. *Tectonics* **2010**, *29*, TC4005. [[CrossRef](#)]
9. Robustelli, G.; Lucà, F.; Corbi, F.; Fubelli, G.; Scarciglia, F.; Dramis, F. Geomorphological Map of the Ionian Area between the Trionto and Colognati River Catchments (Calabria, Italy). *J. Maps* **2009**, *5*, 94–102. [[CrossRef](#)]
10. Robustelli, G.; Lucà, F.; Corbi, F.; Pelle, T.; Dramis, F.; Fubelli, G.; Scarciglia, F.; Muto, F.; Cugliari, D. Alluvial terraces on the Ionian coast of northern Calabria, southern Italy: Implications for tectonic and sea level controls. *Geomorphology* **2009**, *106*, 165–179. [[CrossRef](#)]
11. Ramos, A.; Sopena, A. Gravel bars in low-sinuosity streams. (Permian and Triassic, central Spain). In *Modern and Ancient Fluvial Systems*; Collinson, J.D., Lewin, J., Eds.; Blackwell Scientific, Int. Ass. of Sediment., Special Publication: Palo Alto, CA, USA, 1983; Volume 6, pp. 301–312.
12. Monaco, C.; Tortorici, L.; Paltrinieri, W. Structural evolution of the Lucanian Apennines, southern Italy. *J. Struct. Geol.* **1998**, *20*, 617–638. [[CrossRef](#)]
13. Van Dijk, J.; Bello, M.; Brancaleoni, G.; Cantarella, G.; Costa, V.; Frixia, A.; Golfetto, F.; Merlini, S.; Riva, M.; Torricelli, S.; et al. A regional structural model for the northern sector of the Calabrian Arc (southern Italy). *Tectonophysics* **2000**, *324*, 267–320. [[CrossRef](#)]
14. Faccenna, C.; Becker, T.; Lucente, F.P.; Jolivet, L.; Rossetti, F. History of subduction and back-arc extension in the Central Mediterranean. *Geophys. J. Int.* **2001**, *145*, 809–820. [[CrossRef](#)]
15. Patacca, E.; Scandone, P. Late thrust propagation and sedimentary response in the thrust belt- foredeep system of the Southern Apennines (Pliocene–Pleistocene). In *Anatomy of an Orogen: The Apennines and Adjacent Mediterranean Basins*; Vai, G.B., Martini, I.P., Eds.; Kluwer Academic Publishers: Dordrecht, The Netherlands, 2001; pp. 401–440. [[CrossRef](#)]
16. Chiarabba, C.; De Gori, P.; Speranza, F. The southern Tyrrhenian subduction zone: Deep geometry, magmatism and Plio-Pleistocene evolution. *Earth Planet. Sci. Lett.* **2008**, *268*, 408–423. [[CrossRef](#)]
17. Cifelli, F.; Mattei, M.; Della Seta, M. Calabrian Arc oroclinal bending: The role of subduction. *Tectonics* **2008**, *27*, TC5001. [[CrossRef](#)]
18. Minelli, L.; Faccenna, C. Evolution of the Calabrian accretionary wedge (central Mediterranean). *Tectonics* **2010**, *29*, TC4004. [[CrossRef](#)]
19. Tansi, C.; Muto, F.; Critelli, S.; Iovine, G. Neogene-Quaternary strike-slip tectonics in the central Calabrian Arc (southern Italy). *J. Geodyn.* **2007**, *43*, 393–414. [[CrossRef](#)]
20. Colella, A. Pliocene-Holocene fan deltas and braid deltas in the Crati Basin, southern Italy: A consequence of varying tectonic conditions. In *Fan Deltas: Sedimentology and Tectonic Setting*; Nemeč, W., Steel, R.J., Eds.; Blackie and Son: London, UK, 1988; pp. 50–74.
21. Monaco, C.; Tortorici, L. *Note Illustrative della Carta Geologica d’Italia, Foglio 535 Trebisacce*; ISPRA, Servizio Geologico d’Italia: Roma, Italy, 2008; 104p.
22. Ietto, A.; Ietto, F. *Note Illustrative della Carta Geologica d’Italia, Foglio 543 Cassano allo Ionio*; ISPRA, Servizio Geologico d’Italia: Roma, Italy, 2011; 106p.
23. Michetti, A.M.; Ferrelì, L.; Serva, L.; Vittori, E. Geological evidence for strong historical 807 earthquakes in an “aseismic” region: The Pollino case (Southern Italy). *J. Geodyn.* **1997**, *24*, 67–86. [[CrossRef](#)]
24. Cinti, F.R.; Cucci, L.; Pantosti, D.; D’Addezio, G.; Meghraoui, M. A major seismogenic fault in a ‘silent area’: The Castrovillari fault (southern Apennines, Italy). *Geophys. J. Int.* **1997**, *130*, 595–605. [[CrossRef](#)]
25. Cinti, F.; Moro, M.; Pantosti, D.; Cucci, L.; D’Addezio, G. New constraints on the seismic history 718 of the Castrovillari fault in the Pollino gap (Calabria, southern Italy). *J. Seism.* **2002**, *6*, 199–217. [[CrossRef](#)]
26. Lanzafame, G.; Tortorici, L. La tettonica recente della Valle del fiume Crati (Calabria). *Geogr. Fis. E Din. Del Quat.* **1981**, *4*, 11–21.
27. Filice, F.; Seeber, L. The culmination of an oblique time-transgressive arc continent collision: The Pollino Massif between Calabria and the Southern Apennines, Italy. *Tectonics* **2019**, *38*, 3261–3280. [[CrossRef](#)]
28. Ascione, A.; Cinque, A.; Improta, L.; Villani, F. Late Quaternary faulting within the Southern Apennines seismic belt: New data from Mt. Marzano area (Southern Italy). *Quat. Int.* **2003**, *101–102*, 27–41. [[CrossRef](#)]
29. ISPRA—Dipartimento per il Servizio Geologico d’Italia. Archivio Indagini nel Sottosuolo (Legge 464/84). Available online: <http://sgi2.isprambiente.it/indagini/> (accessed on 12 January 2022).
30. Miall, A.D. *The Geology of Fluvial Deposits: Sedimentary Facies, Basin Analysis and Petroleum Geology*; Springer: New York, NY, USA, 1996; 582p. [[CrossRef](#)]
31. Bridge, J.S. *Rivers and Floodplains*; Blackwell Publishing: Oxford, UK, 2003; 491p.
32. Jo, H.; Chough, S. Architectural analysis of fluvial sequences in the northwestern part of Kyongsang Basin (Early Cretaceous), SE Korea. *Sediment. Geol.* **2001**, *144*, 307–334. [[CrossRef](#)]
33. Vincent, S.J. The Sis palaeovalley: A record of proximal fluvial sedimentation and drainage basin development in response to Pyrenean mountain building. *Sedimentology* **2001**, *48*, 1235–1276. [[CrossRef](#)]
34. Antinao, J.L.; McDonald, E.; Rhodes, E.J.; Brown, N.; Barrera, W.; Gosse, J.C.; Zimmermann, S. Late Pleistocene-Holocene alluvial stratigraphy of southern Baja California, Mexico. *Quat. Sci. Rev.* **2016**, *146*, 161–181. [[CrossRef](#)]

35. Blair, T.C. Cause of dominance by sheetflood vs. debris-flow processes on two adjoining alluvial fans, Death Valley, California. *Sedimentology* **1999**, *46*, 1015–1028. [[CrossRef](#)]
36. Antronico, L.; Greco, R.; Robustelli, G.; Sorriso-Valvo, M. Short-term evolution of an active basin- fansystem, Aspromonte, South Italy. *Geomorphology* **2015**, *228*, 536–551. [[CrossRef](#)]
37. Massari, F.; Parea, G.C. Progradational gravel beach sequences in a moderate- to high-energy, microtidal marine environment. *Sedimentology* **1988**, *35*, 881–913. [[CrossRef](#)]
38. Bluck, B.J. Clast assembling, bed-forms and structure in gravel beaches. *Trans. R. Soc. Edinburgh Earth Sci.* **1999**, *89*, 291–323. [[CrossRef](#)]
39. Zazo, C.; Goy, J.L.; Hillaire-Marcel, C.; Gillot, P.Y.; Soler, V.; González, J.A.; Dabrio, C.J.; Ghaleb, B. Raised marine sequences of Lanzarote and Fuerteventura revisited—A reappraisal of relative sea-level changes and vertical movements in the eastern Canary Islands during the Quaternary. *Quat. Sci. Rev.* **2002**, *21*, 2019–2046. [[CrossRef](#)]
40. Cawthra, H.; Jacobs, Z.; Compton, J.; Fisher, E.; Karkanis, P.; Marean, C. Depositional and sea-level history from MIS 6 (Termination II) to MIS 3 on the southern continental shelf of South Africa. *Quat. Sci. Rev.* **2018**, *181*, 156–172. [[CrossRef](#)]
41. Postma, G. Depositional Architecture and Facies of River and Fan Deltas: A Synthesis. In *Coarse-Grained Deltas*; Colella, A., Prior, D.B., Eds.; Blackwell Publishing Ltd.: Oxford, UK, 1990; Volume 10, pp. 13–28. [[CrossRef](#)]
42. Rasmussen, H. Nearshore and alluvial facies in the Sant Llorenç del Munt depositional system: Recognition and development. *Sediment. Geol.* **2000**, *138*, 71–98. [[CrossRef](#)]
43. Hornung, J.; Asprion, U.; Winsemann, J. Jet-efflux deposits of a subaqueous ice-contact fan, glacial Lake Rinteln, northwestern Germany. *Sediment. Geol.* **2007**, *193*, 167–192. [[CrossRef](#)]
44. Mulder, T.; Alexander, J. The physical character of subaqueous sedimentary density flows and their deposits. *Sedimentology* **2001**, *48*, 269–299. [[CrossRef](#)]
45. Uroza, C.A.; Steel, R.J. A highstand shelf-margin delta system from the Eocene of West Spitsbergen, Norway. *Sediment. Geol.* **2008**, *203*, 229–245. [[CrossRef](#)]
46. Leren, B.L.; Howell, J.; Enge, H.; Martinius, A.W. Controls on stratigraphic architecture in contemporaneous delta systems from the Eocene Roda Sandstone, Tremp-Graus Basin, northern Spain. *Sediment. Geol.* **2010**, *229*, 9–40. [[CrossRef](#)]
47. Winsemann, J.; Hornung, J.; Meinsen, J.; Asprion, U.; Polom, U.; Brandes, C.; Bußmann, M.; Weber, C. Anatomy of a subaqueous ice-contact fan and delta complex, Middle Pleistocene, North-west Germany. *Sedimentology* **2009**, *56*, 1041–1076. [[CrossRef](#)]
48. Sohn, Y.K.; Son, M. Synrift stratigraphic geometry in a transfer zone coarse-grained delta complex, Miocene Pohang Basin, SE Korea. *Sedimentology* **2004**, *51*, 1387–1408. [[CrossRef](#)]
49. Mortimer, E.; Gupta, S.; Cowie, P. Clinoform nucleation and growth in coarse-grained deltas, Loreto basin, Baja California Sur, Mexico: A response to episodic accelerations in fault displacement. *Basin Res.* **2005**, *17*, 337–359. [[CrossRef](#)]
50. Massari, F.; Parea, G.C. Wave-Dominated Gilbert-Type Gravel Deltas in the Hinterland of the Gulf of Taranto (Pleistocene, Southern Italy). In *Coarse-Grained Deltas*; Colella, A., Prior, D.B., Eds.; Blackwell Publishing Ltd., Spec. Publ. Int. Ass. Sedimental.: Oxford, UK, 1990; Volume 10, pp. 311–331. [[CrossRef](#)]
51. Longhitano, S.G. Sedimentary facies and sequence stratigraphy of coarse-grained Gilbert-type deltas within the Pliocene thrust-top Potenza Basin (Southern Apennines, Italy). *Sediment. Geol.* **2008**, *210*, 87–110. [[CrossRef](#)]
52. Massari, F. Upper-flow-regime stratification types on steep-face, coarse-grained, Gilbert-type progradational wedges (Pleistocene, Southern Italy). *J. Sed. Res.* **1999**, *66*, 364–375.
53. Dai Pra, G.; Hearty, P.J. I livelli marini pleistocenici del Golfo di Taranto. Sintesi geocronostratigrafica e tettonica. *Mem. Soc. Geol. Ital.* **1988**, *41*, 637–644.
54. Amato, A.; Belluomini, G.; Cinque, A.; Manolio, M.; Ravera, F. Terrazzi marini e sollevamenti tettonici quaternari lungo il margine ionico dell'Appennino Lucano. *Il Quat. Ital. J. Quat. Sci.* **1997**, *10*, 329–336.
55. Caputo, R. Sea-level curves: Perplexities of an end-user in morphotectonic applications. *Glob. Planet. Chang.* **2007**, *57*, 417–423. [[CrossRef](#)]
56. Waelbroeck, C.; Labeyrie, L.; Michel, E.; Duplessy, J.C.; McManus, J.F.; Lambeck, K.; Balbon, E.; Labracherie, M. Sea-level and deep water temperature changes derived from benthic foraminifera isotopic records. *Quat. Sci. Rev.* **2002**, *21*, 295–305. [[CrossRef](#)]
57. Russo Ermolli, E.; di Pasquale, G. Vegetation dynamics of south-western Italy in the last 28,000 kyr inferred from pollen analysis of a Tyrrhenian Sea core. *Veg. Hist. Archaeobotany* **2002**, *11*, 211–220. [[CrossRef](#)]
58. Buccheri, G.; Capretto, G.; Di Donato, V.; Esposito, P.; Ferruzza, G.; Pescatore, T.; Ermolli, E.R.; Senatore, M.; Sprovieri, M.; Bertoldo, M.; et al. A high resolution record of the last deglaciation in the southern Tyrrhenian Sea: Environmental and climatic evolution. *Mar. Geol.* **2002**, *186*, 447–470. [[CrossRef](#)]
59. Joannin, S.; Ciaranfi, N.; Stefanelli, S. Vegetation changes during the late Early Pleistocene at Montalbano Jonico (Province of Matera, southern Italy) based on pollen analysis. *Palaeogeogr. Palaeoclim. Palaeoecol.* **2008**, *270*, 92–101. [[CrossRef](#)]
60. Breda, A.; Mellere, D.; Massari, F.; Asioli, A. Vertically stacked Gilbert-type deltas of Ventimiglia (NW Italy): The Pliocene record of an overfilled Messinian incised valley. *Sediment. Geol.* **2009**, *219*, 58–76. [[CrossRef](#)]
61. Gobo, K.; Ghinassi, M.; Nemeč, W. Gilbert-type deltas recording short-term base-level changes: Delta-brink morphodynamics and related foreset facies. *Sedimentology* **2015**, *62*, 1923–1949. [[CrossRef](#)]
62. Postma, G. Sea-level-related architectural trends in coarse-grained delta complexes. *Sediment. Geol.* **1995**, *98*, 3–12. [[CrossRef](#)]

63. García-García, F.; Fernández, J.; Viseras, C.; Soria, J.M. Architecture and sedimentary facies evolution in a delta stack controlled by fault growth (Betic Cordillera, southern Spain, late Tortonian). *Sediment. Geol.* **2006**, *185*, 79–92. [[CrossRef](#)]
64. Chiarella, D.; Capella, W.; Longhitano, S.G.; Muto, F. Fault-controlled base-of-scarp deposits. *Basin Res.* **2021**, *33*, 1056–1075. [[CrossRef](#)]
65. Spina, V.; Tondi, E.; Mazzoli, S. Complex basin development in a wrench-dominated back-arc area: Tectonic evolution of the Crati Basin, Calabria, Italy. *J. Geodyn.* **2011**, *51*, 90–109. [[CrossRef](#)]